Biomaterials 33 (2012) 6098–6104

Contents lists available at SciVerse ScienceDirect

Biomaterials

journal homepage: www.elsevier.com/locate/biomaterials

Synergic effects of nanofiber alignment and electroactivity on myoblast differentiation

Sook Hee Ku, Sahng Ha Lee, Chan Beum Park*

KAIST Institute for the BioCentury, Department of Materials Science and Engineering, Korea Advanced Institute of Science and Technology (KAIST), 335 Science Road, Daejeon 305 701, Republic of Korea

ARTICLE INFO

Article history:
Received 2 May 2012
Accepted 10 May 2012
Available online 6 June 2012

Keywords:
Tissue engineering
Myotube formation
Nanofiber alignment
Electrospinning
Conducting polymer

ABSTRACT

The interactions between cells and materials play critical roles in the success of new scaffolds for tissue engineering, since chemical and physical properties of biomaterials regulate cell adhesion, proliferation, migration, and differentiation. We have developed nanofibrous substrates that possess both topographical cues and electroactivity. The nanofiber scaffolds were fabricated through the electrospinning of polycaprolactone (PCL, a biodegradable polymer) and polyaniline (PANi, a conducting polymer) blends. We investigated the ways in which those properties influenced myoblast behaviors. Neither nanofiber alignment nor PANi concentration influenced cell growth and proliferation, but cell morphology changed significantly from multipolar to bipolar with the anisotropy of nanofibers. According to our analyses of myosin heavy chain expression, multinucleate myotube formation, and the expression of differentiation-specific genes (*myogenin*, *troponin T*, *MHC*), the differentiation of myoblasts on PCL/PANi nanofibers was strongly dependent on both nanofiber alignment and PANi concentration. Our results suggest that topographical cues and the electroactivity of nanofibers synergistically stimulate muscle cell differentiation to make PCL/PANi nanofibers a suitable scaffold material for skeletal tissue engineering.

1. Introduction

Cell-materials interaction is a key issue in tissue engineering, because the physicochemical properties of scaffold materials regulate cell behaviors. For decades, researchers have attempted to control cell responses by altering the physicochemical properties of various substances, including their chemical composition, wettability, and topography [1,2]. Designing scaffolds that possess suitable characteristics for specific types of tissues is crucial for achieving actively regenerated tissues. Cells in native tissue are surrounded by an extracellular matrix (ECM), thereby mimicking the features of an ECM is beneficial in efforts to regenerate tissues. Nano-scaled fibrous morphology has been considered one of the main structural characteristics of ECM [3]. To develop ECM-like fibrous structures, electrospinning technology has been utilized because of specific advantages, such as large- scale processing and easy control of fiber diameter or orientation [4–6]. Moreover, the hierarchical structure of ECM fibers (or ECM/cell assembly) is dependent on the specific tissue; for example, well-aligned organization was observed in skeletal muscle tissues, and the alignment of myoblasts is known to be a key step in musculoskeletal myogenesis [7].

Conducting polymers have received a great deal of attention recently, because direct electrical stimulation or electroactivity of substances can influence cellular behaviors. According to the literature, conducting polymers such as polypyrrole (PPy) and polyaniline (PANi) enhanced the growth and differentiation of neurons [8–10], cardiac myoblasts [11,12], and skeletal muscle cells [13,14]. These conducting materials possess a good biocompatibility in vitro as well as in vivo [15–17]. Characteristics of substrates should affect myoblast proliferation and differentiation, but combining the effects of substrate topography and conductivity on myoblast behavior has only rarely been investigated. In this study, we developed nanofibrous substrates exhibiting both aligned morphology and conductivity, and investigated how those properties affect myotube formation. The aligned morphology was controlled through changing the rotation speed of a drum collector during the electrospinning process, and conductivity was provided by blending a conducting polymer and a biodegradable polymer.

2. Materials and methods

2.1. Materials

Polycaprolactone (PCL; Mn = 80,000), polyaniline (PANi; emeraldine base; Mn = 50,000), camphorsulfonic acid (CPSA), gelatin, and dimethylformamide (DMF) were purchased from Sigma–Aldrich (MO, USA), and used without further purification.

* Corresponding author. Tel.: +82 42 350 3340; fax: +82 42 350 3310.
E-mail address: parkcb@kaist.ac.kr (C.B. Park).

0142-9612/$ – see front matter © 2012 Elsevier Ltd. All rights reserved.
doi:10.1016/j.biomaterials.2012.05.018

Table 1
Primer sequences of *myogenin*, *troponin T*, *MHC*, and *beta-actin* for real-time RT-PCR.

Primer	Primer sequence
Myogenin	5′-CTG ACC CTA CAG ACG CCC AC-3′
	5′-TGT CCA CGA TGG ACG TAA GG-3′
Troponin T	5′-TCA ATG TGC TCT ACA ACC GCA-3′
	5′-ACC CTT CCC AGC CCC C-3′
MHC	5′-AGC AGA CGG AGA GGA GCA GGA AG-3′
	5′-CTT CAG CTC CTC CGC CAT CAT G-3′
Beta-actin	5′-AAG GAA GGC TGG AAA AGA GC-3′
	5′-GCT ACA GCT TCA CCA CCA CA-3′

2.2. Preparation of PCL/PANi nanofibers

PCL nanofibers were fabricated by employing an electrospinning process using a rotating drum collector (NanoNC, Korea). PCL solution dissolved in chloroform/DMF (2:1 v/v) and PANi/CPSA solution dissolved in the same solvent were mixed together. The final concentrations of each chemical were as follows: PCL, 200 mg/ml; PANi, 0, 1, 2, or 3 mg/ml; CPSA, the same concentration as PANi. The electrospinning process was carried out with the following parameters: applied voltage, 15 kV; solution feed rate, 10 μl/min; distance between needle and collector, 18 cm; needle size, 21G; rotor speed, 100 rpm for random nanofibers and 900 rpm for aligned nanofibers.

2.3. Characterization of PCL/PANi nanofibers

The resulting nanofibers were observed using scanning electron microscopy (SEM; Hitachi S-4800, Japan), and both the diameter and alignment of nanofibers were analyzed with ImageJ software. The tensile properties of the PCL/PANi nanofibers were analyzed using Instron 5583 (Instron Co., MA, USA). A segment of the nanofiber mesh with 3 cm gauge length and 1 cm width was used for the tests. The strain rate was 10 mm/min and the tests were performed at room temperature. Cyclic voltammograms of the PCL/PANi nanofibers were measured in a 1 M HCl solution with a WMPG 1000 potentiostat/galvanostat (WonATech Co. Ltd., Korea) by using a platinum counter electrode and an Ag/AgCl (3 M NaCl) reference electrode. The cyclic voltammograms were measured in the range of −0.2–0.9 V (vs. Ag/AgCl) at a scan rate of 100 mV/s.

2.4. Cell proliferation and morphology analysis

Mouse skeletal myoblasts C2C12 were maintained in growth media (GM; DMEM containing 10% FBS and 1% antibiotics). Cells were subcultured at least twice a week and were maintained at a humidified atmosphere of 95% air and 5% CO_2. Before cell seeding, PCL/PANi nanofibers were sterilized using a 70% ethanol solution, and were coated with a gelatin solution (0.2 wt% in PBS, pH 7.4) for 30 min at 37 °C for better cell adhesion. C2C12 cells were placed in a 24-well plate at a cell density of 5×10^4 cells/well, and then incubated for 48 h at 37 °C. The cell proliferation on PCL/PANi nanofibers were evaluated using MTT assay. The assay was performed through the following steps: addition of MTT solution (5 mg/ml in PBS, pH 7.4), incubation for 3 h at 37 °C, dissolution of purple formazan using DMSO, and measurement of absorbance at 595 nm. The morphology of cells was analyzed through immunofluorescence study and SEM. For cytoskeleton staining, the cells were fixed with 4% paraformaldehyde, permeabilized with 0.1% Triton X-100, stained with TRICT-phalloidin (Sigma-aldrich, MO, USA), and mounted with Vectashield mounting solution containing DAPI (Vector Laboratories, CA, USA). The actin filaments and nuclei were observed using a fluorescence microscope (Eclipse 80i, Nikon, Japan). For SEM, the cells were fixed with 2.5% gultaraldehyde, washed with PBS and H_2O, and dehydrated in a graded ethanol series.

2.5. Myotube formation analysis with immunocytochemistry

C2C12 cells were seeded at a density of 1×10^5 cells/well and grown in GM for 2 days. To induce myoblast formation, the cells were incubated in differentiation media (DM; DMEM containing 2% horse serum and 1% antibiotics) for further 7 days. DM was changed every other day. After differentiation, the cells were immunostained for myosin heavy chain (*MHC*). The cells were fixed with 4% paraformaldehyde, permeabilized with 0.1% Triton X-100, blocked with 5% BSA solution, incubated with primary antibody (MF20; 1:20; Developmental Studies Hybridoma Bank, IO, USA) at 4 °C overnight, and secondary antibody (Dylight 488-conjugated goat anti-mouse IgG; 1:100; Abcam, UK) at RT for 1 h, and mounted with Vectasheld mouting solution. The morphology of myotubes was observed using a fluorescence microscope, and was analyzed with ImageJ software.

2.6. Quantitative real-time PCR

Real-time RT-PCR was used to analyze the expression level of *Myogenin*, *Troponin T*, and *MHC*. cDNA was directly synthesized from cultured cells using a FastLane cDNA synthesis kit (Qiagen, Germany). Real-time RT-PCR using Quantitect SYBR Green (Qiagen, Germany) was performed with a BioRad CFX96 Real-Time Detection System (Bio-Rad, CA, USA). Thermocycling conditions were as follows: 95 °C for 15 min, 40 cycles of denaturation (15 s, 94 °C), annealing (30 s, 55 °C), and extension (30 s, 72 °C). The primer sequences are listed in Table 1. The relative expression level of each gene as compared to that of *beta-actin* was calculated, and normalized by the value for cells cultured on the random PANi0 fibers.

2.7. Statistical analysis

All of the quantitative results were expressed as mean ± standard error of the mean (SEM). Statistical analysis was carried out by means of one-way analysis of variance (ANOVA). A p-value less than 0.05 was considered statistically significant.

3. Results and discussion

We prepared random or aligned PCL nanofiber matrixes containing polyaniline (PANi), a conducting polymer, to investigate the combined effect of topographical cues and electroactivity on cell behaviors. PANi is a conducting polymer possessing the unique characteristic of tunable conductivity, the doping state of which is easily controlled by acid/base protonation [18,19]. Based on the extremely useful property, PANi has potential applications as a gas sensor [20], actuator [21], and super capacitor [22]. Fig. 1A shows SEM images of randomly oriented or aligned nanofibers with 0, 1, 2, and 3 mg/ml of PANi, which are denoted as PANi0, PANi1, PANi2, and PANi3, respectively. In general, the diameter of electrospun nanofibers is influenced by a number of parameters, including polymer concentration, conductivity, flow rate, and voltage [4]. In this work, the diameter of the nanofibers was reduced through the increasing concentration of PANi due to the increased conductivity of the polymer solution. According to our observation (Fig. 1B), the average diameter of random nanofibers was varied within a range between 280 and 1530 nm, and the diameter decreased with the increasing concentration of PANi. When nanofibers were collected on a drum rotating at a high speed (900 rpm), their average diameters were further reduced to 230–760 nm. Our result is consistent with the literature reporting that nanofiber diameter decreases at high collector rotation speed [23]. The rotation speed affected the orientation of the nanofibers as well as their diameters; as shown in Fig. 1C, over 50% of the nanofibers were aligned within ±10° of the y-axis when they were deposited on a collector rotating at a high speed (900 rpm), while only 15%, approximately, of nanofibers were located in same angle range at a lower speed of rotation (100 rpm).

We further measured various mechanical and electrochemical properties of nanofibers. According to our analysis (Fig. 1D), Young's modulus of randomly oriented nanofibers was measured in the range of 2.27–2.79 MPa, not dependent on PANi concentration. In contrast, Young's modulus was significantly increased when the nanofibers were aligned; for example, tensile modulus of aligned nanofibers for PANi0 and PANi3 was as high as 24.4 and 34.6 MPa, respectively. Tensile properties of nanofibers can be enhanced with alignment, because tensile force distributes to all fibers equally when the load is applied parallel to the fiber direction [24]. The differences in the tensile modulus of aligned PANi0, 1, and 2 nanofibers were not statistically significant. We attribute the variation in the mechanical properties of aligned PANi3 compared to aligned PANi0 to the blending of more brittle PANi into elastic PCL [13]. We analyzed the electrochemical properties of PCL/PANi nanofibers by using cyclic voltammetry (Fig. 1E). PANi-containing nanofibers exhibited significant peaks at 0.24 V and 0.76 V during the oxidation cycle, which corresponds to lecuoemeraldine/emeraldine and emeraldine/pernigraniline transitions, respectively [25]. With the increasing concentration of PANi in the PCL/PANi nanofibers, we observed a gradual increase in the intensity and integration of voltammetric peaks. Note that the integration of a cyclic voltammogram is associated with redox charge of material [19,26].

These results imply that conductivity of PANi-blended nanofibers increased with the PANi concentration [26,27].

To investigate the effects of conductivity and topographical cues on myogenic differentiation, we seeded C2C12 mouse myoblasts on random or aligned PCL/PANi nanofiber scaffolds. After 2 days of growth, cell viability was similar for all tested nanofibers, according to the results of MTT assay (Fig. 2A). This implies that neither the concentration of PANi nor the anisotropy of nanofibers influence

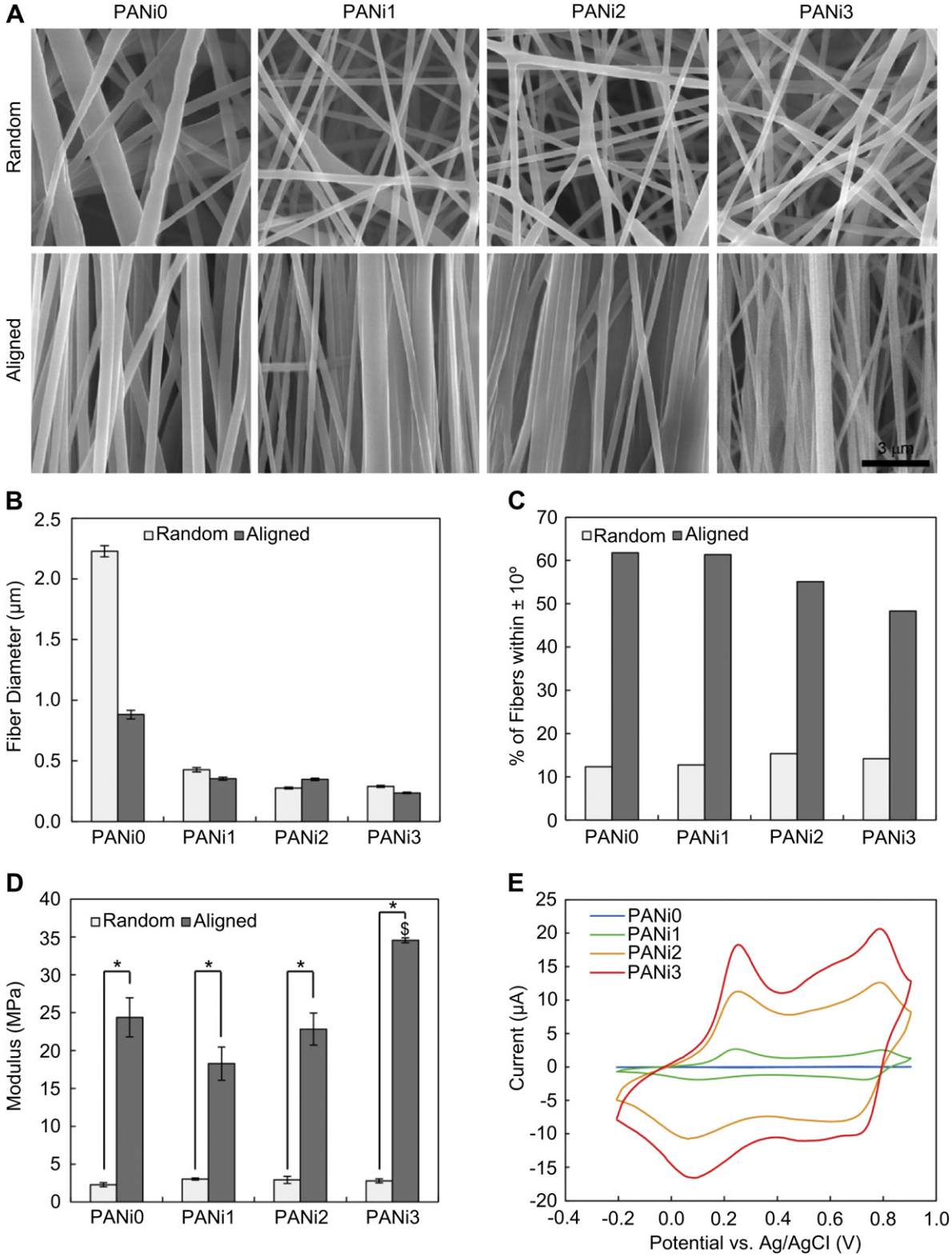

Fig. 1. (A) SEM images and (B) average diameters of PCL/PANi nanofibers. (C) Percentage of nanofibers aligned within $\pm 10^{\circ}$ of *y*-axis. (D) Young's modulus and (E) cyclic voltammograms for PCL/PANi nanofibers. * indicates a significant difference in comparison with random nanofibers at the same concentration of PANi ($p < 0.05$). $ denotes a significant difference compared to aligned PANi0 nanofibers ($p < 0.05$).

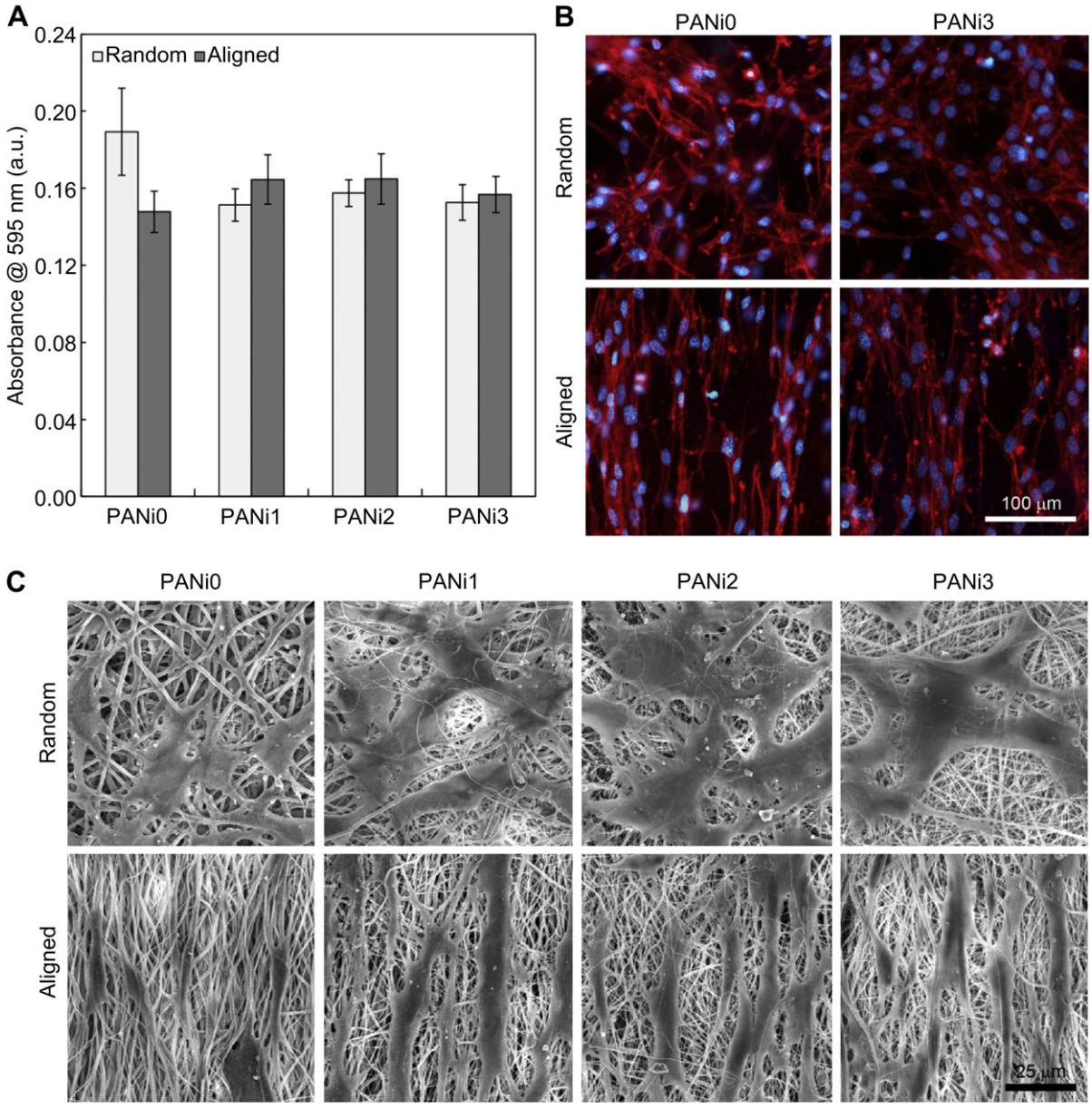

Fig. 2. (A) Cell proliferation on PCL/PANi nanofibers, measured by MTT assay. Cell morphology analyzed through (B) immunofluorescence staining for actin and (C) SEM. C2C12 cells were grown in growth media for 2 day.

cell growth and proliferation. We observed morphologies of cells grown on PANi/PCL nanofibers by using cytoskeleton staining and a scanning electron microscope (Fig. 2b and C). The cells grown on randomly oriented nanofiber matrixes showed flat and multipolar morphologies, while cells adhered to individual nanofibers with bipolar morphologies when grown on aligned nanofibers. The concentration of PANi did not significantly affect the morphology of cells. To investigate myogenic differentiation on PANi/PCL nanofibers, we cultured C2C12 cells in differentiation media (DMEM containing 2% horse serum) for 7 days, and then stained for myosin heavy chain (*MHC*), a protein required for myotube formation. As shown in Fig. 3A, C2C12 cells expressed *MHC* on all nanofiber samples, but total *MHC*-positive area differed depending on both PANi concentration and nanofiber alignment (Fig. 3B). On randomly oriented nanofibers, total *MHC*-positive area per 10^5 μm^2 increased from 14700 μm^2 for PANi0 to 25500, 25800, and 32200 μm^2 for PANi1, 2, and 3, respectively. Additionally, a greater area was stained as *MHC*-positive when cells were cultured on an aligned nanofiber matrix: 13800, 34300, 35500, and 42100 μm^2 for PANi0, 1, 2, and 3, respectively. For PANi-blended nanofibers, cells on *aligned* nanofibers expressed approximately 1.3-fold more *MHC* compared to those on *random* nanofibers at the same concentration of PANi in the nanofiber. As shown in Fig. 3C, the number of myotubes formed on PCL/PANi nanofibers also increased with the PANi concentration and nanofiber alignment: 5.54, 7.45, 8.25, and 9.59 myotubes per 10^5 μm^2 on random PANi0, 1, 2, and 3; 5.50, 9.81, 10.28, and 11.69 myotubes per 10^5 μm^2 on aligned PANi0, 1, 2, and 3. Our results suggest that both conductivity and alignment of nanofibers can synergistically stimulate myogenic differentiation.

We analyzed the morphology of myotubes that were formed on PANi/PCL nanofiber scaffolds. According to our results (Fig. 4A), the alignment of nanofibers significantly influenced the growth direction of myotubes; while only approximately 10–20% of myotubes were located within $\pm 10^\circ$ of the *y*-axis when formed on random

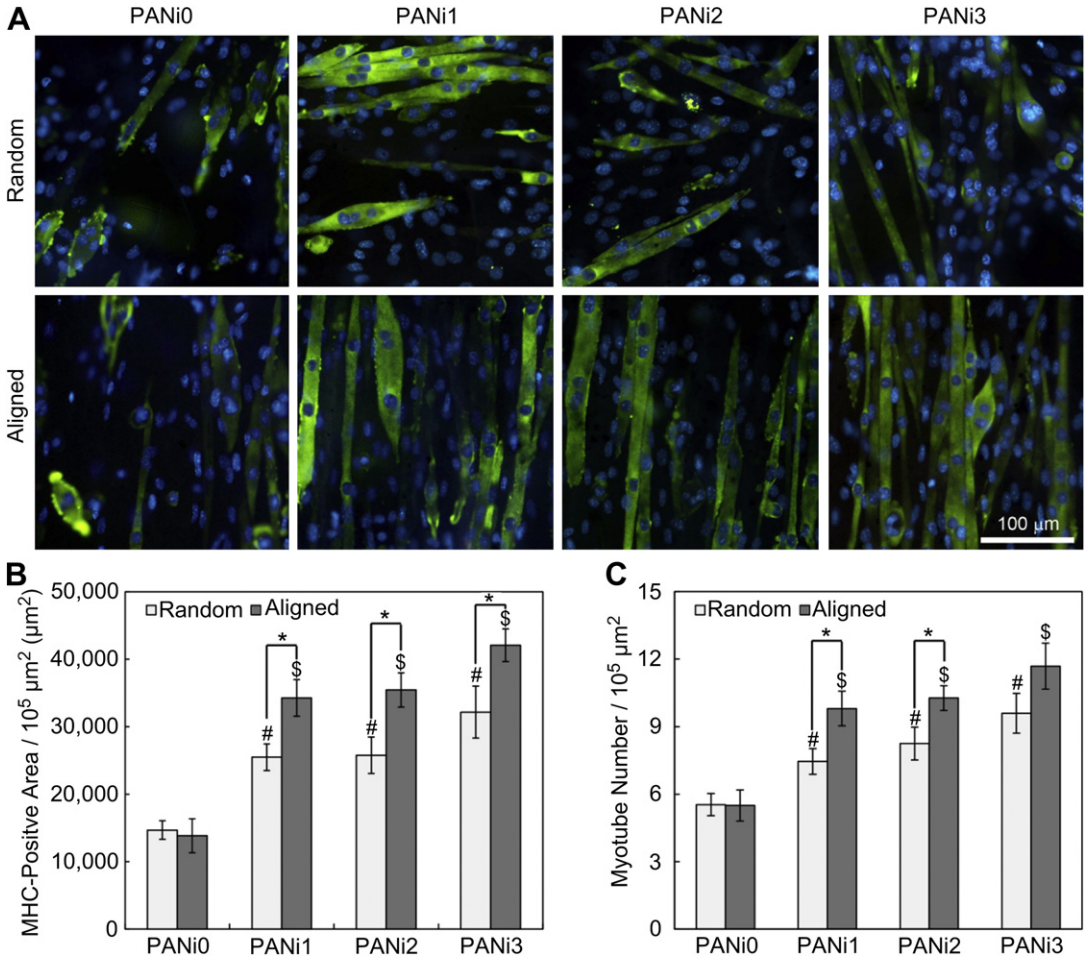

Fig. 3. (A) Immunofluorescence staining for myosin heavy chain (*MHC*). (B) Quantitative analysis of total *MHC*-positive area and (C) myotube number per 10^5 μm^2. Cells were grown in growth media for 2 days and then incubated in differentiation media for 7 days. * indicates a significant difference in comparison with random nanofibers at the same concentration of PANi ($p < 0.05$). # and $ denote a significant difference compared to random and aligned PANi0 nanofibers, respectively ($p < 0.05$).

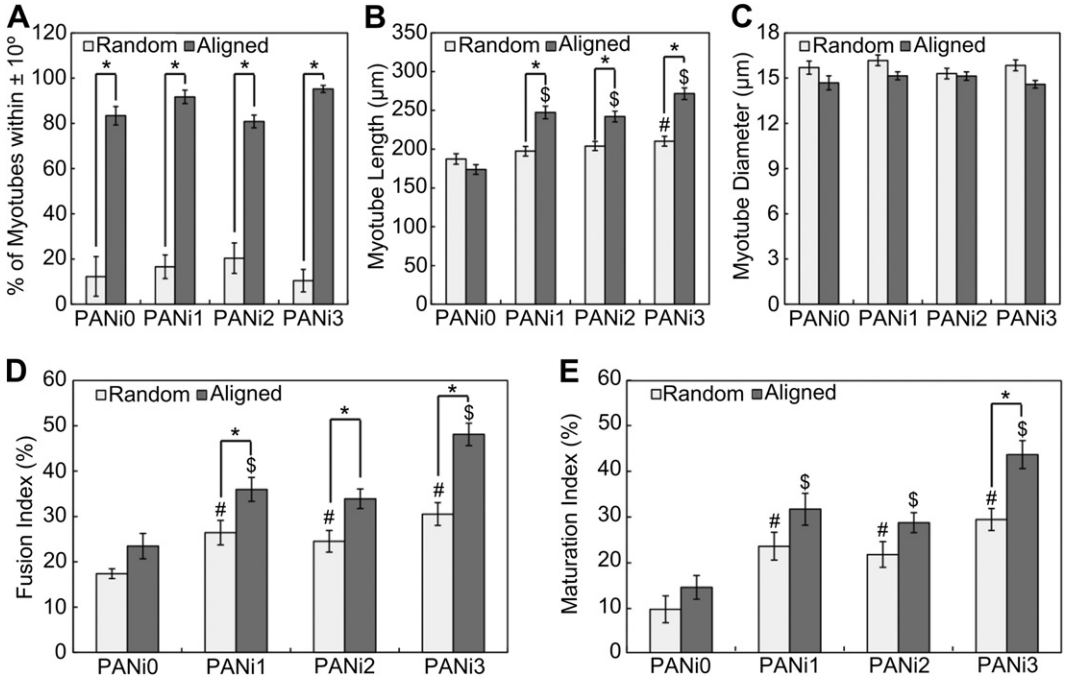

Fig. 4. (A) Percentage of myotubes aligned within ±10° of nanofiber axis. Quantification of (B) myotube length and (C) diameter, (D) fusion index (ratio of the nuclei number in myocytes with two or more nuclei to the total nuclei number), and (E) maturation index (% myotubes with ≥5 nuclei). * indicates a significant difference in comparison with random nanofibers at the same concentration of PANi ($p < 0.05$). # and $ denote a significant difference compared to random and aligned PANi0 nanofibers, respectively ($p < 0.05$).

nanofibers, more than 80% of myotubes aligned within the same angle range when grown on an aligned nanofiber matrix. In contrast, PANi concentration negligibly affected the myotube alignment. The length of myotubes was also influenced by both PANi concentration and nanofiber alignment (Fig. 4B). On randomly oriented nanofibers, myotubes were 187.3, 197.4, 204.1, and 210.2 μm long on PANi0, 1, 2, and 3, respectively. The lengths of myotubes changed to 173.9, 247.2, 242.1, and 271.5 μm when formed on aligned PANi0, 1, 2, and 3, respectively. The lengths of myotubes increased 1.2–1.3-fold for aligned nanofibers only when the nanofibers contained PANi. In contrast to myotube length, the diameter of myotubes was irrespective of PANi concentration or nanofiber alignment (Fig. 4C).

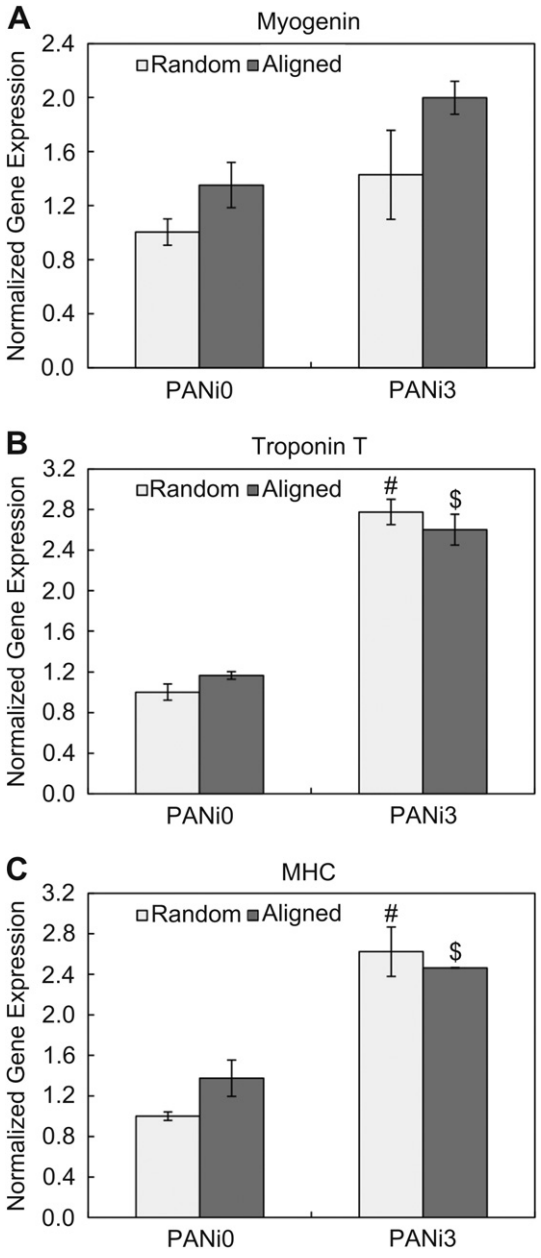

Fig. 5. Myogenic gene expression. (A) *Myogenin*, (B) *Troponin T*, and (C) *MHC*. Gene expression was analyzed after 2 days growth following 7 days differentiation. # and $ denote a significant difference compared to random and aligned PANi0 nanofibers, respectively ($p < 0.05$).

C2C12 myoblasts fuse together to form multinucleate myotubes when cultured in differentiation media [28]. We calculated the fusion index to quantify the myoblast differentiation by determining the ratio of nuclei number in the *MHC*-positive region having more than 2 nuclei to the total number of nuclei according to the literature [29]. As shown in Fig. 4D, the fusion index increased from 17% for PANi0 to 30% for PANi3 for randomly oriented nanofibers. The cells on aligned nanofibers increased the fusion index by approximately 1.3–1.6-fold of those on random fibers at the same concentration of PANi. We further calculated the maturation index as a differentiation parameter by measuring the percent of myotubes with more than 5 nuclei [29]. Like the fusion index, the maturation index also increased with PANi concentration from 9% for random PANi0 to 29% for random PANi3, and from 14% for aligned PANi0 to 43% for aligned PANi3 (Fig. 4E). Nanofiber alignment also enhanced the maturation index approximately 1.3–1.5-fold. Our results show that myoblast fusion and myotube maturation were stimulated by both substrate electroactivity and topographical cues.

We further quantified the gene expression levels of myogenesis-specific markers by reverse transcription PCR analysis. Three genes, *myogenin*, *troponin T*, and *MHC*, were used as indicators for early, late, and fully differentiated stages, respectively. *Myogenin* is a muscle-specific transcription factor and expressed before the establishment of the post-mitotic state [28]. *Troponin T* and *MHC* are major components of the contractile muscle fibers [30,31]. As shown in Fig. 5, the expression of *myogenin*, *troponin T*, and *MHC* genes was increased with PANi blending and nanofiber alignment. The normalized expression level on aligned PANi3 was 2.0, 2.6, and 2.5-fold higher than that on random PANi0 for *myogenin*, *troponin T*, and *MHC* genes, respectively. Taken together, PCL/PANi nanofibers synergistically stimulate myogenic differentiation induced by electroactivity and topography.

4. Conclusion

We developed a nanofibrous substrate possessing both aligned morphology and conductivity, and investigated the effects of these properties on myoblast growth and myotube formation. According to our results, skeletal myoblasts grew well on PCL/PANi nanofibers irrespective of PANi concentration or fiber alignment, but their morphology was highly dependent on the fiber alignment. Myotube formation was significantly affected by both PANi concentration and nanofiber alignment according to the *MHC* expression level, fusion/maturation index, and gene (*myogenin*, *troponin T*, and *MHC)* expression levels. Our work suggests that PCL/PANi nanofibers are suitable scaffold material for skeletal tissue engineering, enhancing myoblast attachment, proliferation, and myogenic differentiation.

Acknowledgments

This study was supported by grants from the National Research Foundation (NRF) via National Research Laboratory (R0A-2008-000-20041-0), Converging Research Center (2009-0082276), and Intelligent Synthetic Biology Center of Global Frontier Project (2011-0031957).

References

[1] Ma PX. Biomimetic materials for tissue engineering. Adv Drug Del Rev 2008; 60:184–98.
[2] Shin H, Jo S, Mikos AG. Biomimetic materials for tissue engineering. Biomaterials 2003;24:4353–64.

[3] Mccullen SD, Ramaswamy S, Clarke LI, Gorga RE. Nanofibrous composites for tissue engineering applications. WIREs Nanomed Nanobiotech 2009;1:369–90.
[4] Pham QP, Sharma U, Mikos AG. Electrospinning of polymeric nanofibers for tissue engineering applications: a review. Tissue Eng 2006;12:1197–211.
[5] Huang Z-M, Zhang YZ, Kotaki M, Ramakrishna S. A review on polymer nanofibers by electrospinning and their applications in nanocomposites. Composites Sci Technol 2003;63:2223–53.
[6] Teo W, Ramakrishna S. A review on electrospinning design and nanofibre assemblies. Nanotechnology 2006;17:R89.
[7] Wakelam M. The fusion of myoblasts. Biochem J 1985;228:1.
[8] Xie J, Macewan MR, Willerth SM, Li X, Moran DW, Sakiyama-Elbert SE, et al. Conductive core-sheath nanofibers and their potential application in neural tissue engineering. Adv Funct Mater 2009;19:2312–8.
[9] Liu X, Yue Z, Higgins MJ, Wallace GG. Conducting polymers with immobilised fibrillar collagen for enhanced neural interfacing. Biomaterials 2011;32:7309–17.
[10] Schmidt CE, Shastri VR, Vacanti JP, Langer R. Stimulation of neurite outgrowth using an electrically conducting polymer. Proc Natl Acad Sci U S A 1997;94:8948.
[11] Bidez PR, Li S, Macdiarmid AG, Venancio EC, Wei Y, Lelkes PI. Polyaniline, an electroactive polymer, supports adhesion and proliferation of cardiac myoblasts. J Biomater Sci Polym Ed 2006;1:199–212.
[12] Borriello A, Guarino V, Schiavo L, Alvarez-Perez M, Ambrosio L. Optimizing pani doped electroactive substrates as patches for the regeneration of cardiac muscle. J Mater Sci Mater Med 2011;22:1053–62.
[13] Jun I, Jeong S, Shin H. The stimulation of myoblast differentiation by electrically conductive sub-micron fibers. Biomaterials 2009;30:2038–47.
[14] Gilmore KJ, Kita M, Han Y, Gelmi A, Higgins MJ, Moulton SE, et al. Skeletal muscle cell proliferation and differentiation on polypyrrole substrates doped with extracellular matrix components. Biomaterials 2009;30:5292–304.
[15] Humpolicek P, Kasparkova V, Saha P, Stejskal J. Biocompatibility of polyaniline. Synth Met 2012;162:722–7.
[16] Ateh DD, Navsaria HA, Vadgama P. Polypyrrole-based conducting polymers and interactions with biological tissues. J R Soc Interface 2006;3:741–52.
[17] Mattioli-Belmonte M, Giavaresi G, Biagini G, Virgili L, Giacomini M, Fini M, et al. Tailoring biomaterial compatibility: in vivo tissue response versus in vitro cell behavior. Int J Artif Organs 2003;26:1077.
[18] Heeger AJ. Semiconducting and metallic polymers: the fourth generation of polymeric materials (nobel lecture). Angew Chem Int Ed 2001;40:2591–611.
[19] Barbero C, Miras M, Kötz R, Haas O. Comparative study of the ion exchange and electrochemical properties of sulfonated polyaniline (SPAN) and polyaniline (PANI). Synth Met 1993;55:1539–44.
[20] Virji S, Huang J, Kaner RB, Weiller BH. Polyaniline nanofiber gas sensors: examination of response mechanisms. Nano Lett 2004;4:491–6.
[21] Baker CO, Shedd B, Innis PC, Whitten PG, Spinks GM, Wallace GG, et al. Monolithic actuators from flash-welded polyaniline nanofibers. Adv Mater 2008;20:155–8.
[22] Ryu KS, Kim KM, Park N-G, Park YJ, Chang SH. Symmetric redox supercapacitor with conducting polyaniline electrodes. J Power Sources 2002;103:305–9.
[23] Lee H, Yoon H, Kim G. Highly oriented electrospun polycaprolactone micro/nanofibers prepared by a field-controllable electrode and rotating collector. Appl Phys Mater Sci Process 2009;97:559–65.
[24] Baji A, Mai Y-W, Wong S-C, Abtahi M, Chen P. Electrospinning of polymer nanofibers: effects on oriented morphology, structures and tensile properties. Composites Sci Technol 2010;70:703–18.
[25] Shin YJ, Kim SH, Yang DH, Kwon H, Shin JS. Amperometric glucose biosensor by means of electrostatic layer-by-layer adsorption onto polyaniline-coated polyester films. J Ind Eng Chem 2010;16:380–4.
[26] Hung CC, Wu CH, Yang CH, Wei Y, Wen TC. Poly (vinyl alcohol)-assisted dispersion of polyaniline nanofiber for electrochemical applications. J Mater Res 2011;26:2980.
[27] Namazi H, Kabiri R, Entezami A. Determination of extremely low percolation threshold electroactivity of the blend polyvinyl chloride/polyaniline doped with camphorsulfonic acid by cyclic voltammetry method. Eur Polym J 2002;38:771–7.
[28] Andrés V, Walsh K. Myogenin expression, cell cycle withdrawal, and phenotypic differentiation are temporally separable events that precede cell fusion upon myogenesis. J Cell Biol 1996;132:657–66.
[29] Bajaj P, Reddy B, Millet L, Wei C, Zorlutuna P, Bao G, et al. Patterning the differentiation of C2C12 skeletal myoblasts. Integr Biol 2011;3:897–909.
[30] Charge SBP, Rudnicki MA. Cellular and molecular regulation of muscle regeneration. Physiol Rev 2004;84:209–38.
[31] Meriane M, Roux P, Primig M, Fort P, Gauthier-Rouvière C. Critical activities of Rac1 and Cdc42Hs in skeletal myogenesis: antagonistic effects of JNK and p38 pathways. Mol Biol Cell 2000;11:2513–28.